

## DATA ASSIMILATION AND DYNAMICAL INTERPOLATION IN GULFCAST EXPERIMENTS

ALLAN R. ROBINSON, MICHAEL A. SPALL, LEONARD J. WALSTAD  
and WAYNE G. LESLIE

*Division of Applied Sciences, Harvard University, Cambridge, MA 01238 (U.S.A.)*

(Received April 25, 1988; revised September 20, 1988; accepted October 4, 1988)

### ABSTRACT

Robinson, A.R., Spall, M.A., Walstad, L.J. and Leslie, W.G., 1989. Data assimilation and dynamical interpolation in GULFCAST experiments. *Dyn. Atmos. Oceans*, 13: 301–316.

GULFCAST is a forecast system for the Gulf Stream meander and ring region consisting of a dynamical open-ocean model and an observational network comprised of remotely sensed sea-surface temperatures (and recently, sea-surface height) and critically located air-dropped expendable bathythermographs (AXBTs). We present here the case study of a real-time forecast system carried out for 2 weeks in the Spring of 1986 during the development of GULFCAST methodology. The AXBT data from successive flights were assimilated and a frontal location was 'nowcast' and forecast within the error bounds of navigation, AXBT sampling and model resolution during a multiple ring–stream interaction event.

### INTRODUCTION

The Gulf Stream meander and ring (GSMR) region lies to the east of Cape Hatteras and to the south of the Grand Banks, extending to about 50°W longitude. Eastward the flow weakens, branches and breaks off filaments as it develops into the Gulf Stream extension and North Atlantic current systems. Within the GSMR region, the Gulf Stream is a powerful and well-formed free jet, which, with little change of axial profile, snakes along a well defined but contorted path that varies energetically with time. Meanders and waves grow and propagate, loops intensify and snap off into cold and warm core rings. Typically, the region is populated by several rings; warm cores trapped in the alley between the stream and the continental rise to the north and cold cores roaming more freely south of the stream and into the Sargasso Sea. Ring–stream and ring–ring interactions occur, reabsorption by coalescence is often the fate of a ring and multiple ring–stream interactions occur. The energetic GSMR region is interesting

dynamically, important practically and accessible to remote sensing. The phenomena described above are, within the ocean, the counterpart of atmospheric weather phenomena. We have established a system for forecasting the internal weather of the sea in the GSMR region called GULFCAST.

Data assimilation is recognized by ocean scientists to be a general methodology of great potential for dynamical studies and essential for efficient and feasible ocean prediction (Mooers et al., 1987). Four-dimensional data assimilation in meteorology and numerical weather forecasting, and the theoretical basis of optimal field estimation procedures (Ghil, 1988) provide guidance to ocean dynamicists as they develop their dedicated methods. Data assimilation is essentially a systematic field estimation procedure where observational estimates are melded with dynamical model estimates via some weighting procedure. To us it seemed natural, initially, to adopt an engineering approach in order to bring to bear oceanographic experience to the complex real fields of interest, in the context of a new situation involving dynamical model initializations with real but limited data. The procedure involves subjective weights in the melding of dynamical model output and non-uniform surface and subsurface temperature observations in the estimation of the temperature fronts associated with the jet's axis and the ring currents. These frontal locations are then used to reinitialize the dynamical model via a 'feature-model' method, and thus to enable the advance of the forecast in time.

The GULFCAST system was set up (Robinson et al., 1987) during the period November 1985 to November 1986, and since that time has been providing weekly research forecasts on a regular basis (Glenn et al., 1987). As initially set up the system's components were a dynamical model consisting of the Harvard quasi-geostrophic open-ocean model, and an observational network consisting of satellite-observed infra-red (IR) sea-surface temperatures (SST) together with occasional dedicated and designed air-dropped expendable bathythermographs (AXBT) flights. During the period November 1985 to June 1986 we developed methodology, calibrated the model and established the validity of GULFCAST concepts through a series of five real-time forecast experiments in subregions of the GSMR region. This paper presents a case study of the most extensive of these experiments carried out from 19 May to 6 June 1986.

Considering the GSMR phenomena introduced in the first paragraph, it is reasonable to expect forecast verification, both qualitatively and quantitatively, to depend upon phenomenological regimes. A 'propagation regime' in which pre-existing features develop and translate is dynamically different and simpler than an 'interaction regime' (Robinson, 1987, Chapter 2) in which an energetic synoptical-dynamical event is taking place. We use the term synoptical-dynamical event for interactions between rings and/or

rings and the stream, which can drastically alter frontal locations rapidly. These include ring births and reabsorptions by the stream, ring mergers, etc. In both regimes, but especially the latter, it is data assimilation that can control phase error and yield frontal forecasts of the practical accuracy  $O(10\text{ km})$  useful for operational forecasting. The experiments of the set-up period (Robinson et al., 1987) indicated the capability of the GULFCAST system to achieve this accuracy with adequate AXBT data. The case illustrated here involves a multiple ring-stream interaction.

## 2. CONTEXT AND METHODOLOGY

Because the phenomena of interest exist over large spatial scales in the Gulf Stream meander and ring region, it is not economically feasible to obtain the data necessary for the traditional approach of objectively mapping the fields from a grid of observations, as we have done previously for model initializations in the POLYMODE (Carter and Robinson, 1987) and California Current regions (Robinson et al., 1986). The dynamical model is baroclinic and quasi-geostrophic with open boundary conditions (Robinson and Walstad, 1987). However, the fact that the Gulf Stream region contains individual, identifiable energetic features may be exploited to initialize the model with only limited data sets, i.e., segments of the fronts associated with the stream and rings. The method, called 'feature-model initialization', is presented in Robinson et al. (1988), to which the reader is referred for details. When viewed in the stream coordinates, the Gulf Stream always looks more or less the same all along its meandering path. The Gulf Stream and its associated rings have characteristic properties regarding their shape, size, structure and strength. Feature models, analytic representations of these structures with tuning parameters, have been designed based on historical data. The parameters for the Gulf Stream are maximum velocity at the surface, base of the thermocline, and bottom,  $e$ -folding width of the stream, and depth of the base of the thermocline. The ring parameters are maximum velocity, maximum radius, radius of maximum velocity, maximum depth and vertical shear. The feature-model initialization undergoes a three-phase evolution during model integration. These phases are dynamical adjustment of the features, dynamical interpolation between the features, and dynamical evolution of the fields. The analytic features first make slight dynamical adjustments during the model integration but with the structures remaining largely unchanged. The motionless water between the features spins up through the process of dynamical interpolation and at the same time the vorticity interactions among the features begin. Near-field circulations are established after about a day of integration. Dynamical evolution then occurs as the features interact and evolve in accordance with the

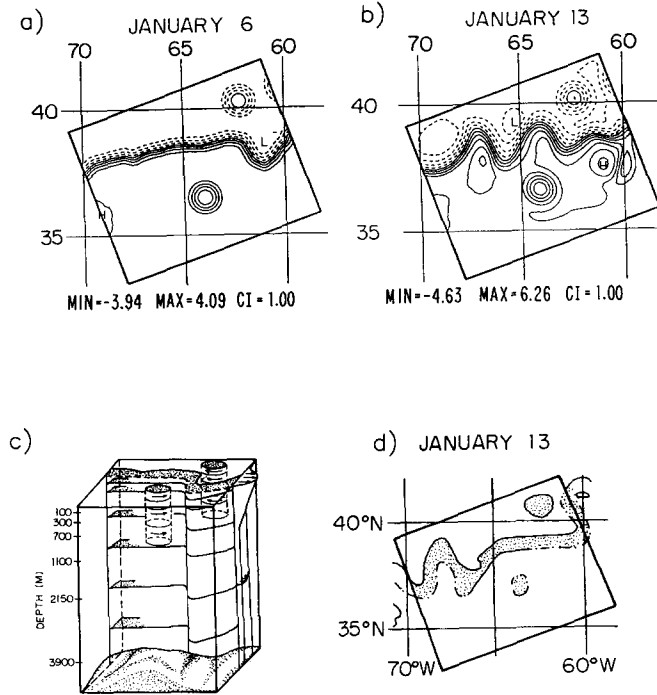


Fig. 1. (a) 100-m streamfunction field for quasi-geostrophic (QG) model initialization on January 6, 1986. (b) 100-m streamfunction forecast for January 13, 1986. (c) Three-dimensional feature-model initialization. (d) January 13, 1986 Gulf Stream north wall and ring position from satellite IR.

dynamical model. The feature models represent initialization fields only, subsequent fields of course have the structure as determined by the quasi-geostrophic model and its computational grid.

An initial condition with the feature models hung beneath the IR images for January 6, 1986 is shown in Fig. 1a and c. The stream is flat over most of the region with a slight dip near 62°W. Figure 1 shows (b) the actual real-time 7-day model forecast with persisted boundary conditions, and (d) satellite IR for that day. A dramatic development of a large double meander has occurred and was predicted by the dynamical model 1 week prior to the actual event. Further experiments show that using the observed boundary conditions for the feature inflow/outflow gives even closer agreement with the IR. This real-time forecast provided a good example of the dynamical model's ability to deal with energetic and non-obvious developments. The capability of the model to make realistic rings is treated in detail in Robinson et al. (1988) and a real-time forecast of an unusual large ring is illustrated by Glenn et al. (1987).

Satellite sea-surface temperature images (IR) were available in each of the five forecast experiments to test and develop real-time forecasting capabilities in the GSMR region and AXBTs were available for four out of the five experiments. These two data sources complement each other well; the satellite IR gives surface thermal front information with large spatial coverage and the AXBTs give temperature profiles down to about 400 m at specific points. The IR is a very good tool to define large-scale structures of the Gulf Stream and rings from the strong thermal signature at the surface. However, satellite IR gives no data over clouded regions and may give misleading information in regions of surface warming or cooling. Cold rings often lose their surface signature because of atmospheric forcing, but still have very strong subsurface fields. Large patches of warm water are seen on the slope side of the stream, which hint at the presence of a warm ring but have no deep structure at all. Because the AXBTs can locate the subsurface thermal signature of the Gulf Stream and warm and cold rings, they have a dual role in model initialization and verification. They may be used to determine if questionable surface features seen in the IR have any deep structure and to locate very accurately the position and strength of critical features already known to exist, and to search for features, such as cold rings, that may have covered over and lost their surface signal. A great deal of information can be obtained from a limited number of AXBTs by using satellite IR and dynamical model calculations to plan efficient and effective flight tracks. Direct aerial mapping with a regular grid would require one or two orders of magnitude larger number of probes.

The GULFCAST system, consisting of the model together with IR and occasional dedicated AXBT observations, was tested under a wide range of circumstances. The phenomena that were predicted by the forecasting procedure included Gulf Stream meander growth and propagation, straightening out a previously meandering stream, ring formations, and ring-stream interactions and movements (Robinson et al., 1987). The model domains ranged from  $720 \times 720 \text{ km}^2$  to  $1200 \times 900 \text{ km}^2$  and were located from the inlet region near  $70^\circ \text{W}$  out to  $58^\circ \text{W}$ . A total of 23 model forecasts were conducted; ranging from 4 days to 1 week in duration. A total of 12 AXBT flights were flown during these exercises, of which 11 gave information useful for model verification. Fifteen north-wall positions were determined from the AXBT data sets. The difference between the predicted and measured location of the north wall was found to be  $< 10 \text{ km}$  in 10 of the 15 comparisons. Three of the remaining five comparisons showed 10-km differences. The remaining two locations were off by 20 and 60 km; the latter being influenced by a poor inflow boundary condition. The tendencies observed in the IR images were reproduced in all regions where there was no cloud cover; very good agreement was seen three out of four times. Errors

associated with 'north wall' frontal location are due to possible navigation error 0 (1 km), AXBT interpretation (sampling interval about 20 km), or definition of the north wall in model forecasts (model grid usually 15 km). Satellite IR is not used for precise location of the north wall because atmospheric forcing can shift the surface signature by tens of kilometers, but it is useful to define the larger scale tendencies of the flow.

These experiments contributed to the development of our real-time forecasting methodology for the GSMR region, summarized here for the case of starting a new forecast. Ambiguities in the initial condition are removed through a combined analysis of dynamical model calculations, repeated AXBT flights and satellite IR. First, IR, AXBT data and previous model forecasts are used to define and position the feature models for initialization. This forecast is run in both a large domain,  $O(2000 \times 1000 \text{ km}^2)$ , on a supercomputer, and in a subregion,  $O(1000 \times 1000 \text{ km}^2)$  or less, on a local microcomputer. The subregion run serves as a central forecast for a matrix of sensitivity runs in which the initial condition is varied to determine which features are most critical to the evolution of the flow field. The AXBT flight tracks are then designed to locate those features, taking into account trade-offs between horizontal resolution, spatial coverage, feature location and vulnerability to equipment failure. The dynamical model is reinitialized with a composite analysis of (1) AXBT data, (2) model runs and (3) satellite data. Boundary conditions for the real-time forecast are provided either by (i) estimating new feature positions using forward time extrapolation of meanders and rings by a simple propagation speed or by (ii) interpolating information from the large domain supercomputer run. With the uncertainties of the region now lessened and the features better defined, the model forecasts the flow fields ahead in time. New AXBT flights should be executed to locate critical flow indices (i.e., crests, troughs, ring-stream interactions) for both model verification and reinitialization of the next set of real-time forecasts.

The dynamical model has several uses in this scheme. It is first used to determine the most critical features that must be located with AXBT flights via the sensitivity runs. Secondly, the supercomputer run is used to get boundary conditions for subregion forecasts from the approximate forecast in the larger domain. Most importantly the model dynamically interpolates the data both horizontally between the features and vertically beneath the features as well as projecting its evolution ahead in time. Dynamical interpolation produces smooth three-dimensional dynamically consistent fields of the quantities of interest ('nowcast' and forecasts). Benchmark hindcasting (Robinson et al., 1988) indicates that the dynamical model can evolve fields forward in time for 2–4 weeks, passing through more than one synoptical–dynamical event.

## 3. THE GULFCAST EXPERIMENT 19 MAY TO 6 JUNE 1986

This experiment is presented in some detail, because, as the major effort during the developmental phase of GULFCASTing, it was of 3 weeks duration, had adequate associated AXBT resources and effectively utilized all elements of the methodology described above. An attempt was made to achieve an accurate forecast of the location of the Gulf Stream front, i.e., not only to represent correctly events and features, but to control phase error via the data assimilation approach. This was accomplished successfully for a section of the stream and in an interesting situation in which a multiple ring–stream interaction was occurring.

The experiment was a start-up situation that was initiated via the NOAA IR SST for 19 May, which is shown in Fig. 2a. Additional IR data were utilized for 28 May (Fig. 2b), but not after that time as the later stages of this GULFCAST were carried out at sea and the IR data were not available

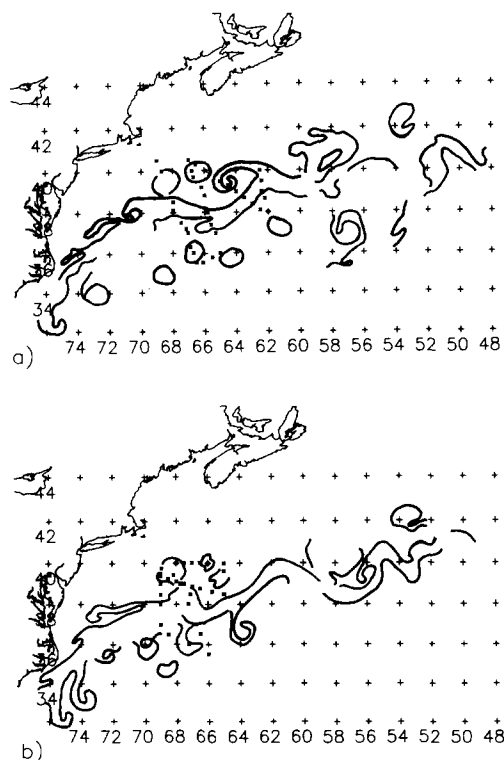
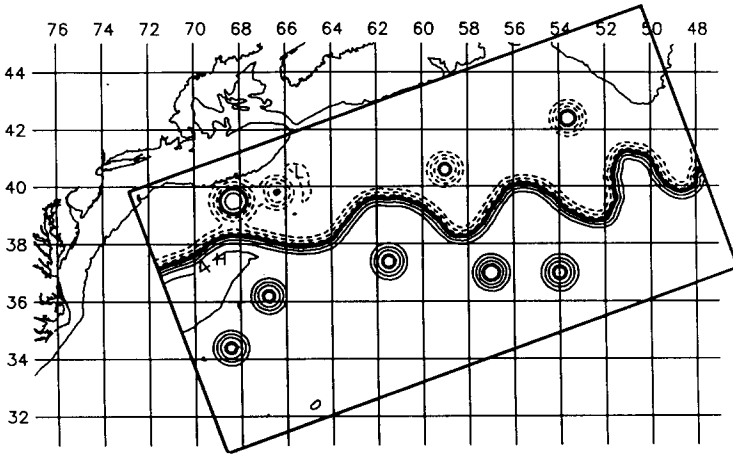
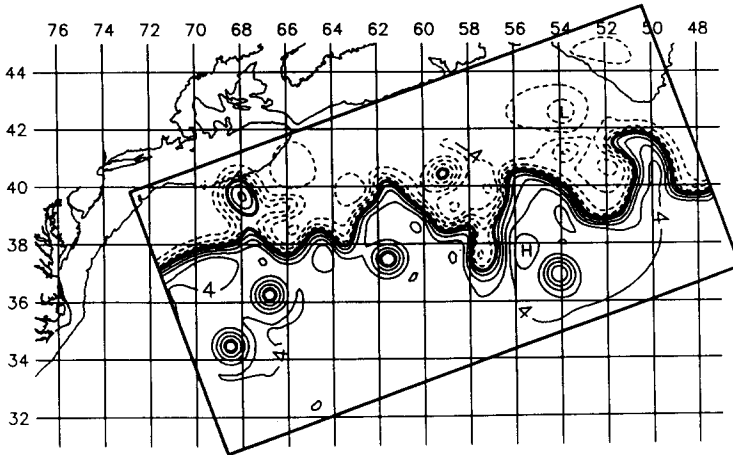


Fig. 2. (a) Gulf Stream fronts and ring positions for May 19, 1986 and AXBT positions for May 23, 1986. (b) Gulf Stream fronts and ring positions for May 28, 1986 and AXBT positions for May 29, 1986. Front and ring positions are determined from satellite IR.



a) Initialization : 19 May 1986



b) 7 Day Forecast : 26 May 1986

Fig. 3. (a) 100-m streamfunction field for supercomputer forecast. (b) 100-m streamfunction field after a 7-day forecast.

in real time. The starting GULFCAST region was large, extending from 48 to 72°W longitude (Fig. 3), but was reduced in size to 64–72°W for the final accurate forecast attempt for 6 June. This latter, approximately 800-km<sup>2</sup> region, was also used for extensive sensitivity forecast experiments (see Fig. 5) and sampled by AXBTs. Dedicated AXBT flights were carried out on 23 and 29 May (Fig. 2) and four additional stream crossings were obtained by AXBTs, for updating and verification, two each on 2 and 6 June.

The jet and ring frontal information contained in the two IR maps of Fig. 2 is fortuitously good. Solid lines indicate observed surface frontal features,



and dotted lines indicate information from previous data for regions that were cloud covered or featureless (according to standard NOAA convention). On 19 May, to the east of  $72^\circ$  W longitude, there are four meander crests, six cold eddies, and five warm eddies indicated. As usual we are concerned with whether or not the surface eddies correspond to thermocline rings, the location of thermocline fronts relative to surface indicators and the usefulness of past information and subjective interpretations. These questions are especially demanding at start-up time. The new information revealed by the IR of 28 May are: the deepening of the meander trough at  $67^\circ$ , eastward propagation of some long-wave feature between  $65^\circ$  and  $55^\circ$ , the development of a sharp feature at  $53^\circ$ , and definite surface signals of the two cold eddies centered on  $64^\circ$  and  $67^\circ$  W longitude.

The large domain forecast carried out on the CRAY XMP at NRL was initialized with six levels and 15 km resolution via the interpretation of the 19 May data shown in Fig. 3a. There are four warm and five cold rings present. The cold ring at  $64^\circ$  W should of course have been included, but the omission of the warm eddy at  $65^\circ$  will be shown to be correct. The forecast 1 week ahead shows the evolution of features as displayed on Fig. 3b. The two warm rings in the west and the stream are mutually interacting. The smaller ring is being absorbed by the larger ring, which is in contact with the stream. The stream is distorting into a pattern that includes a deepening trough at  $66^\circ$  W and also one at  $63^\circ$  (in the vicinity of the missing ring). Further downstream, meanders steepen and propagate eastward and the cold ring at  $57^\circ$  has attached.

The interaction of the stream and the two warm rings can be identified as the critical synoptical-dynamical event controlling the frontal location and evolution in the western half of the domain, and a careful definition of the interaction was attempted. The first AXBT flight was designed on the basis of the first forecast, as seen on the nominal track of Fig. 4a, to locate the two warm rings relative to the stream, to investigate the possible existence of a third warm ring, to locate similarly one cold ring, and to position and determine the shape of the current by four crossings. The subsurface fields of velocity and temperature predicted by the model along the first section of the track are shown on Fig. 4b. Realistic fields have filled in by dynamical interpolation and evolved by 23 May from the feature-model initialization of 19 May. Typical signatures of features are shown on Fig. 4c from sample AXBTs; all profiles obtained for this experiment are reported in Robinson et al. (1987).

The AXBT flight, as actually carried out on 23 May, consisted of 34 drops with only two failures in the pattern shown on Fig. 2a. All the objectives of the flight were successfully accomplished except that technical difficulties occurred in the region between  $38.5^\circ$  N  $68.0^\circ$  W and  $40.0^\circ$  N  $68.7^\circ$  W, thus

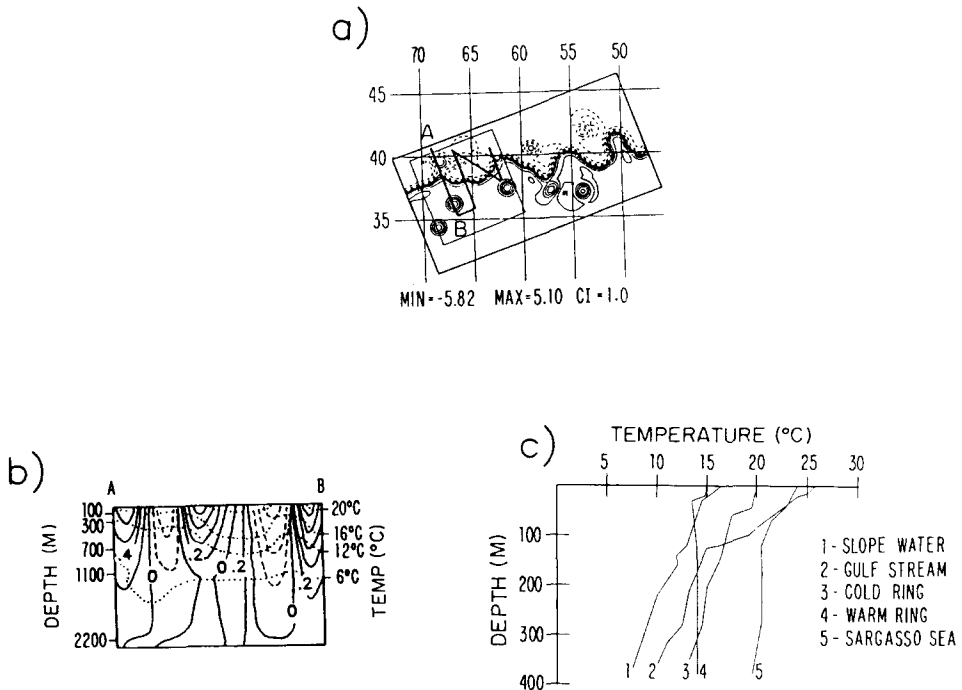


Fig. 4. (a) 100-m streamfunction field from supercomputer forecast for May 23, 1986; domain for subregion forecasts (light line); AXBT flight track (heavy line). (b) velocity and temperature section along line A-B of (a). Velocity contour interval is  $0.2 \text{ m s}^{-1}$ ; temperature contour interval is  $4^\circ \text{C}$ . (c) Sample AXBT temperature profiles.

failing to quantify accurately the major stream-ring relationship or interaction in the most critical region. At the time of this flight and subsequently, the sensitivity experiments (Fig. 5) to be discussed below were being performed and analyzed. On the basis of those results, together with the new IR SST (Fig. 2b) and the results of the first flight, the second flight was designed and flown (Fig. 2b) with 27 drops and only one failure. The main objectives were to locate the positions of the two warm rings relative to each other and the stream and, additionally, to locate a nearby cold ring that could possibly enter into a mutual interaction. These were successfully accomplished. The information concerning features and frontal locations from all the flights is presented in Table I and on Fig. 6, which also summarizes the ring signals indicated by the IR.

The situation with respect to the cold rings in the region was ambiguous on 19 May, but was clarified by strong signals for all three rings on the 28 May. Additionally, ring  $C_1$  was located on each of the first two AXBT flights. The two stream crossings indicated in Table I on June 2 were accomplished by a flight pattern down  $69^\circ \text{W}$  and up  $72^\circ \text{W}$ , which were

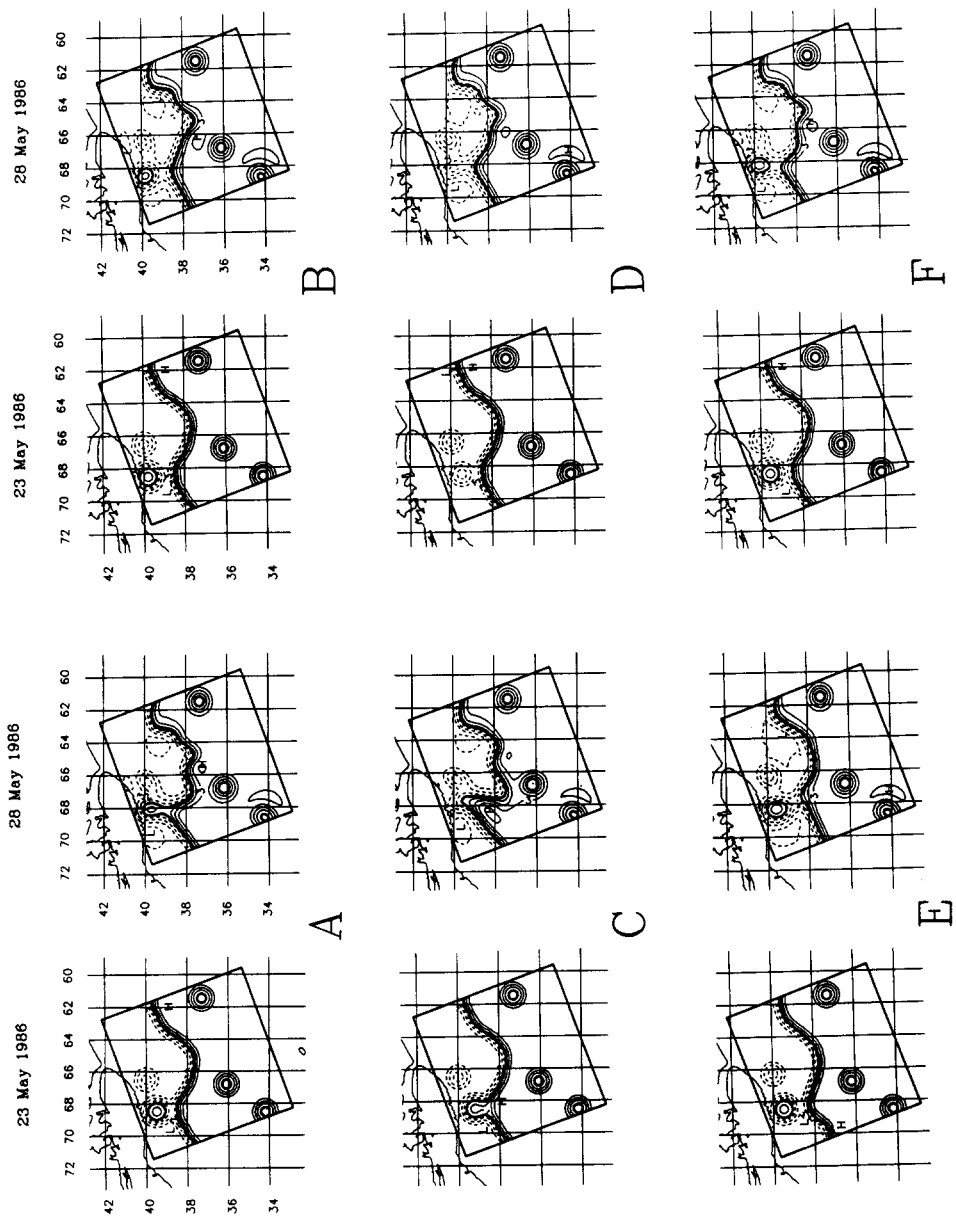


Fig. 5. Initialization and 7-day forecast 100-m streamfunction fields for six sensitivity forecasts performed in the subregion shown in Fig. 4a.

TABLE I  
Gulf Stream Frontal Locations (North Wall) by AXBTs

Date	23-5-86	23-5	23-5	23-5	29-5	29-5
Latitude (° N)	38.8	39.7	> 37.4, < 38.7	> 38.5	38.2	38.2
Longitude (° W)	63.8	62.5	66.0	68.0	69.0	67.2
Date	29-5	2-6	2-6	6-6	6-6	
Latitude (° N)	< 38.5	38.5	> 37.0, < 39.0	37.9	38.2	
Longitude (° W)	65.0	69.0	72.0	70.4	68.9	

The notation  $\leq$  indicates a bound, e.g., on 23-5 at 68.0° W the Gulf Stream was determined to be located to the north of 38.5° N.

connected by a track along 34.5° N. This flight was seeking evidence of another cold ring, however none were found. The warm-ring picture was quite complicated and the interpretation presented schematically in Fig. 6 was evolved with some difficulty in real time, and involved interpretative input from the dynamical model runs. We believe the model initialization of 2 June for the final forecast to have been unambiguous and reasonably

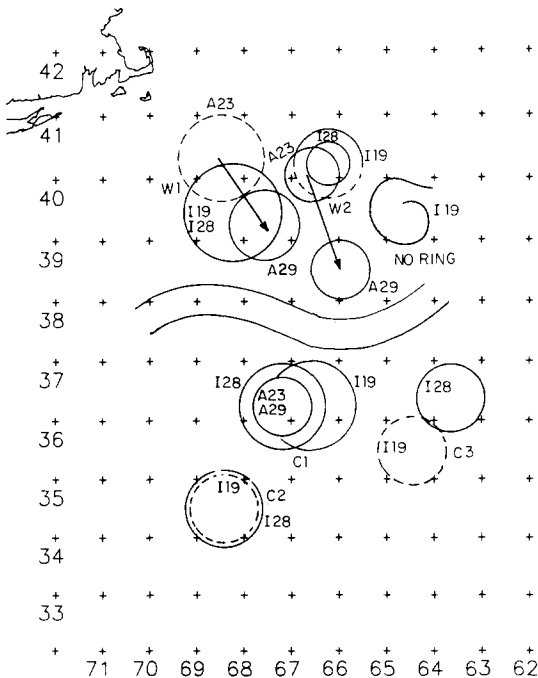


Fig. 6. Schematic interpretation of ring and stream positions as determined from satellite IR, AXBTs and dynamical forecasts.

accurate. The flight of 23 June gave some indication of a ring centered to the north of the surface IR signal of 19 June at  $68.5^\circ\text{W}$ , definitely located a ring in the vicinity of the partial IR surface signal near  $66.5^\circ\text{W}$  and showed that the feature at  $65.0^\circ\text{W}$ , which had a definite surface signal in AXBTs, did not extend to thermocline depth. Both  $W_1$  and  $W_2$  were well located on the flight of 29 June.  $W_2$  moved to the south by southeast by just under 200 km in 6 days, indicating a speed of  $\sim 30\text{ km day}^{-1}$  ( $\sim 35\text{ cm s}^{-1}$ ). The data for  $W_1$  are not as good, but it appeared to move to the eastsoutheast at perhaps a comparable but somewhat slower speed. Both speeds and directions are unusual and indicate an interaction event. The stream crossings in Table I are consistent with the interaction event and are useful in the interpretation of the sensitivity forecast and in the context of the IR frontal segment estimates.

The matrix of sensitivity forecasts was carried out for a set of model initializations designed on the basis of all information available following the immediate analysis of the May 23 AXBT data. The overall objectives were: to determine the range of stream- $W_1$ - $W_2$  (hereafter referred to as  $S$ - $W_1$ - $W_2$ ) interactions consistent with this information base, to anticipate the magnitude of frontal shifts that could be induced by the interaction in the next few days, and to assess possible critical data requirements for the next AXBT flight. The major parameter studied was the exact location of  $W_1$  relative to the stream but the size of  $W_1$  and the stream shape were also

TABLE II  
Sensitivity forecasts for stream- $W_1$ - $W_2$  interaction

Run	Initial condition	Ring evolution	Stream evolution
A	Central forecast. $W_1$ partially attached	$W_1 \rightarrow \text{NE}$ $W_2 \rightarrow \text{S}$ $W_1$ coalescing $W_1$ - $W_2$ begin merger	Trough develops at $67^\circ\text{W}$ crest at $68.5^\circ\text{W}$
B	Weak interaction. $W_1$ separated to N	$W_1$ stationary $W_2$ slightly $\rightarrow \text{S}$	straightens from $68$ to $65^\circ\text{W}$
C	Strong interaction. $W_1$ overlapping Stream	$W_1$ rapidly $\rightarrow \text{SE}$ $W_1 \rightarrow \text{S}$ $W_1$ fully absorbed $W_2$ coalescing	sharp meander N-S front along $68^\circ\text{W}$ deep trough at $67^\circ\text{W}$
D	Weak interaction. Small $W_1$ , grazing	$W_1 \rightarrow \text{E}$ $W_2$ stationary	stationary
E	Weak interaction. Stream to S from $68$ to $70^\circ\text{W}$	$W_1$ slightly $\rightarrow \text{E}$ $W_2$ slightly $\rightarrow \text{S}$	straightens from $68$ to $70^\circ\text{W}$
F	Intermediate interaction. $W_1$ grazing	$W_1 \rightarrow \text{NE}$ $W_2 \rightarrow \text{S}$	small amplitude waves from $68.5$ to $65^\circ\text{W}$

varied. The runs are summarized in Table II and the initial (23 May) and final (28 May) states are shown in Fig. 5.

Examination of the results indicate that interaction of  $W_1$  and the stream leads to an eastward advection of  $W_1$ , which can also have either a northward or a southward component, depending upon where the advection occurs or 'grabs hold' relative to the meander crest initially at  $68.5^\circ\text{W}$ . Strong interaction leads to complete coalescence or absorption of  $W_1$  by the stream. Eastward movement of  $W_1$  favors interaction with  $W_2$ , and since  $W_1$  is considerably stronger than  $W_2$ , the initial stage is a southward advection of  $W_2$  by  $W_1$ . The ultimate development of a strong interaction is not illustrated here but should be dependent upon phasing of the three-way  $S$ - $W_1$ - $W_2$  interaction, i.e., either merger of  $W_1$  and  $W_2$  could occur (case D) followed by coalescence of the larger ring, or  $W_2$  could coalesce with the stream following absorption of  $W_1$  (case C). The flight pattern of Fig. 2b pinned down the ring-stream system on 29 May. The movements to the southeast schematized on Fig. 6 indicate an interaction intermediate between runs A and C, i.e., strong enough for southeast advection of  $W_1$  but not for absorption.

The final forecast in this series was carried out from 2 to 4 June 1986 in a domain shifted slightly to the west, as shown in Fig. 7. The initialization (Fig. 7a) was the best estimate of the fields possible obtained by synthesizing the information available from the IR of the 28 May, and the AXBTs from 29 May and dynamical model results. The initialization was prepared via dynamical adjustment and interpolation from 29 May, which matched the

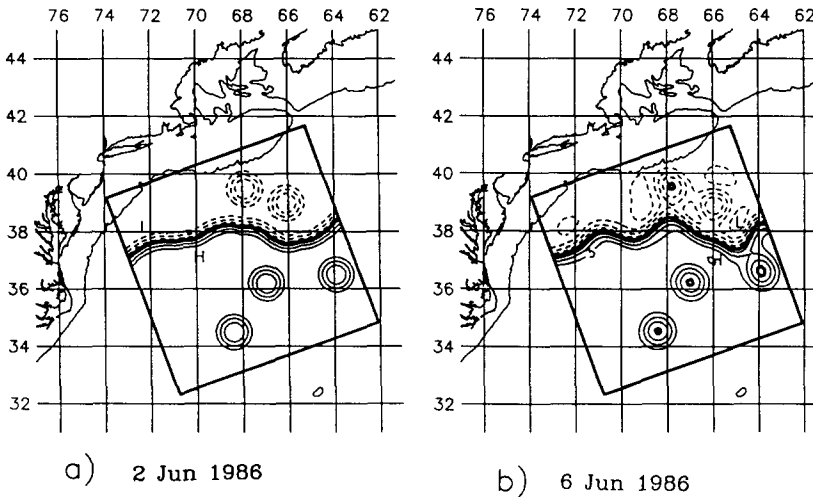


Fig. 7. (a) 100-m streamfunction field for initialization of final forecast beginning June 2, 1986. (b) 100-m streamfunction field forecasted for June 6, 1986.

stream crossings of 2 June and included cold ring  $C_3$  first observed in the IR of 28 May. The forecast (Fig. 7b) is seen to involve a three-way type of grazing 'advective' interaction among  $S-W_1-W_2-S$ . This is accompanied by a deep looping distortion of the stream to the south (trough at  $65^\circ W$ ), which initiates an additional interaction with  $C_3$ . There is also growth of a 300-km wave in the west of the domain. The distortion of the stream associated with the  $S-W_1-W_2-S-C_3$  interaction event has shifted the Gulf Stream frontal position by almost 100 km in 4 day around  $65^\circ W$  and shifts of 30–50 km occur along the stream. These magnitudes are of considerable practical consequence. The two stream frontal locations available for verification of 6 June (Table I) agree with the forecast locations within  $< 10$  km, which is the limit of resolution for the location of the north wall of the front by interpolation, associated both with the AXBT estimate (sampling grid ( $\sim 25$  km)) and the model estimate (horizontal grid, 15 km).

#### 4. CONCLUSIONS

We exercised the GULFCAST system of dynamical model, frontal segments in sea-surface temperature obtained from satellite IR, and dedicated, designed AXBT flights in the Gulf Stream Meander and Ring region from start-up on the 19 May until 6 June 1986. We carried out a series of 'nowcasts' and forecasts which, via data assimilation, improved to the point where verification flights agreed with a few days prediction within error bounds of resolution resulting from navigation, AXBT sampling and model resolution. This experiment together with similar results from four related experiments in the period November 1985 to June 1986 indicated (i) the applicability of the Harvard open-ocean quasi-geostrophic model to Gulf Stream and ring system forecasts, and (ii) the ability of the system to achieve accuracies that are useful practically when adequate in situ data are available for assimilation. This is valid for both periods of meander propagation and growth and for energetic synoptical–dynamical events. The data requirements are, of course, less in the former case.

The success of these experiments led to the establishment of an ongoing and continuous GULFCAST research–operational forecast system at Harvard in November of 1986. Weekly forecasts are carried out for 1 week ahead. The continued ability of the GULFCAST system to predict synoptical–dynamical events is demonstrated. GEOSAT altimetric data have been added to the observational network, and a surface boundary layer model is being attached to the quasi-geostrophic model (Walstad, 1987) to allow more accurate assimilation of satellite IR SST. A scheme for the continuous melding of observed frontal segments into ongoing dynamical model runs is

being developed in order to replace the less appropriate reinitializations that are presently used for assimilations.

#### ACKNOWLEDGMENTS

We acknowledge the help of Dr Arthur J. Mariano in providing selected relevant historical data for use during the May–June experiment at sea, of Mr Ralph Milliff for technical and logistical support, and Ms Marsha Glass Cormier for essential arrangements. This research was supported by the Office of Naval Research under Contract No. N00014-84-C-0461 for Ocean Dynamics and the analysis was partially supported by the Oceanographer of the Navy through NORDA (Contract No. N00014-86-K-6002).

#### REFERENCES

- Carter, E.F. and Robinson, A.R., 1987. Analysis models for the estimation of oceanic fields. *J. Atmos. Ocean. Techn.*, 4 (1): 49–74.
- Ghil, M., 1988. Meteorological data assimilation for oceanographers. *Dyn. Atmos. Oceans*, submitted.
- Glenn, S., Robinson, A.R. and Spall, M.A., 1987. Recent results from the Harvard Gulf Stream Forecasting Program. *Oceanographic Monthly Summary*, vii(4). NOAA, Washington, DC.
- Mooers, C.M.K., Robinson, A.R. and Thompson, J.D. (Editors), 1987. *Ocean Prediction Workshop 1986: A Status and Prospectus Report on the Scientific Basis and the Navy's Needs*. Institute for Naval Oceanography, NSTL, MS., 486 pp.
- Robinson, A.R., 1987. Predicting open ocean currents, fronts and eddies. In: J.C.J. Nihoul and B.M. Jamart (Editors), *Three Dimensional Ocean Models of Marine and Estuarine Dynamics*. Elsevier, Amsterdam, pp. 89–112.
- Robinson, A.R. and Walstad, L.J., 1987. The Harvard open ocean model: calibration and application to dynamical process forecasting and data assimilation studies. *J. Appl. Numer. Math.*, 3 (1–2): 89–131.
- Robinson, A.R., Carton, J.A., Pinardi, N. and Mooers, C.N.K., 1986. Dynamical forecasting and dynamical interpolation: an experiment in the California current. *J. Phys. Ocean.*, 16: 1561–1579.
- Robinson, A.R., Spall, M.A., Leslie, W.G., Walstad, L.J. and McGillicuddy, D.J., 1987. *Gulfcasting: dynamical forecast experiments for Gulf Stream rings and meanders November 1985–June 1986*. Harvard University Reports in Meteorology and Oceanography, No. 22.
- Robinson, A.R., Spall, M.A. and Pinardi, N., 1988. Gulf Stream simulations and the dynamics of ring and meander processes. *J. Phys. Oceanogr.*, 18: 1811–1853.
- Walstad, L.J., 1987. *Modelling and forecasting deep ocean and near surface mesoscale eddies: hindcasting and forecasting with, and coupling a surface boundary layer model to, the Harvard quasi-geostrophic model*. Ph.D. Thesis, Harvard University Reports in Meteorology and Oceanography, No. 23.